Int J Clin Exp Med 2018;11(7):6560-6570
www.ijcem.com /ISSN:1940-5901/IJCEM0076542

Original Article

Qualitative analysis of axon regeneration by semi-automatic programs on axon photomicrographs proven through concepts of calculus

Feng Li[1*], Zhen Zhang[2*], Xue Wang[2], Zhujun Feng[1], Heng Xu[3], Shaoqing Feng[3], Kan Wang[4], Airong Ma[1], Jun Chen[5,6], Yan Wo[1]

[1]Department of Anatomy and Physiology, School of Medicine, Shanghai Jiao Tong University, Shanghai City, China; Departments of [2]Dermatology, [3]Plastic and Reconstructive, Shanghai Ninth People's Hospital, Shanghai Jiao Tong University School of Medicine, Shanghai City, China; [4]Institute of Nano Biomedicine and Engineering, Department of Instrument Science and Engineering, Key Lab. for Thin Film and Microfabrication Technology of Ministry of Education, School of Electronic Information and Electronic Engineering, Shanghai Jiao Tong University, Shanghai City, China; [5]Department of Orthopaedic Sports Medicine, Huashan Hospital, Fudan University, Shanghai City, China; [6]CAS Key Laboratory of Nano-Bio Interface, Suzhou Institute of Nano-Tech and Nano-Bionics, Chinese Academy of Sciences, Suzhou, Jiangsu Province, China. [*]Equal contributors.

Received March 22, 2018; Accepted May 13, 2018; Epub July 15, 2018; Published July 30, 2018

Abstract: Objective: Manual counting and measuring of axon counts, axon calibers, and g-ratios are time consuming and can be biased by observer variation. Methods: This study introduces a quick, reproducible, and semi-automatic method for screening eligible graphs from the mass image using Image Pro Plus software, objectively defining the image to be analyzed and further clarifying the research object by manual assistance while excluding images that do not meet standards. This method was compared with the manual method using toluidine blue samples of nerve transections. Results: There were no significant differences for axon counts, axon calibers, or axon g-ratios between semi-automatic and manual methods. Pearson's correlation coefficient for axon calibers or axon g-ratios, from both methods, showed no statistically significant differences. Bland-Altman image analysis showed similar results for axon counts obtained by two methods. The time taken by semi-automatic analysis was less than that taken by manual identification. Conclusion: In conclusion, this semi-automatic method is accurate and rapid compared to the traditional manual method.

Keywords: g-ratio, homothetic morphometry, semi-automatic, manual measurement, sciatic nerve

Introduction

Several established routine parameters, such as axon counts, axon calibers, and g-ratios, have been reliable indices for assessing axonal myelination [1, 2]. Myelination is produced by the myelin sheath which has an essential impact on structure, function, and physiology, as well as on the surrounding matrix. Thus, to appropriately evaluate, routine parameters of axon regeneration are utilized to describe the relationship between biophysical properties of axonal structure and function with remyelination in the process of nerve regeneration [3-5].

Measurement of parameters in axon regeneration of peripheral nerves in rats can be evaluated by manual, automatic, and semi-automatic methods. Until now, the dominant method has been the manual one [6]. There are previously established and fixed protocols [7, 8]. However, the manual morphometric analysis of an entire peripheral nerve (700-800 myelinated fibers) requires an entire day's work [9]. Manual measurements have usually been described as tedious, time consuming, difficult to perfectly handle, and subject to many sources of errors when many nerve histology parameters were to be measured. Automatic methods, having the advantage of being fast, efficient, and relatively affordable, have been suggested to analyze data [10, 11]. However, automatic techniques have shown some errors due to the software's inability to separate clustered fibers in a perfect fashion, eventually producing chro-

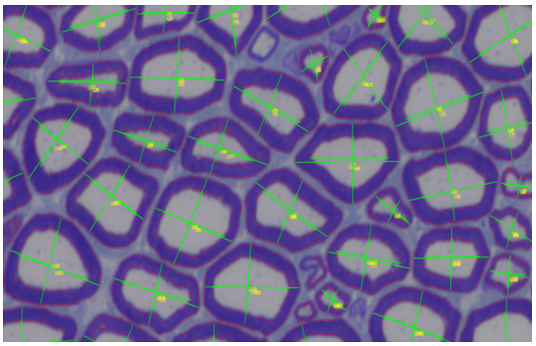

Figure 1. Manual axon g-ratio measurement. Axon caliber and fibers outer diameter can be measured by using Image Pro analyzer software. 160 ×.

matic aberrations in images [12-14]. This is because of the threshold factor which leads to mismatch. Artefactual images, like blood vessels and perineurial fragments, will also lead to errors. Observer bias and pix of images are also interference factors for automatic methods [9, 15]. To compensate for possible errors in measurements, manual intervention is sometimes necessary. Therefore, the combination of manual and automatic methods, meaning semi-automatic analysis, is now one of the most common approaches for peripheral nerve morphometry. With the aid of semi-automatic axon analysis system, data collection and analysis have improved in efficiency along with maintaining a high level of accuracy.

This present study describes an efficient, effective, and translatable semi-automatic method of peripheral nerve morphometry. Axon counts, axon calibers, and g-ratios from rat sciatic nerves were determined, using semi-automatic and the manual method. Statistical comparison of values from both methods revealed significantly similar results, while the resources (time, work load) required for the semi-automatic method were significantly less.

Materials and methods

Experimental design

This study used 34 three-month-old female Sprague-Dawley rats, weighing 300 g to 320 g. All procedures were approved by the Care and Use of Laboratory Animals Institute of Shanghai, China. Experiments were carried out with approval from the Animal Experimentation Ethics Committee of School of Medicine, Shanghai Jiao Tong University, Shanghai, China. All animals were raised in a carefully regulated environment maintained at 21-25 degree Celsius, 40-70% relative humidity, and 12/12 hour light/dark cycle. They received tap water and normal rat chow ad libitum. The rodents underwent exposure and transection of the sciatic nerve at mid-thigh. The contralateral side was used as the control side, without any treatments. Wounds were closed by 4-0 nylon sutures. Animals were then euthanized by intraperitoneal administration of 0.4% sodium pentobarbital at 100 mg/kg body weight at the end of the study.

Histologic samples

Both sides of the rats underwent the following testing procedures: approximately 0.5 cm of site of injury was removed and fixed overnight in 4% paraformaldehyde/(2.5% glutaraldehyde) solution. Nerves were cut transversally with 0.5 μm, stained in 1% sodium borate with 0.1% toluidine blue, 0.1% azure II, and 0.1% methylene blue solution and observed under a light microscope (× 40) (LEICA DM6000B, Lecia Microsystems, Germany).

Manual measurement of axon parameters

One photomicrograph of the whole nerve transverse section was obtained with 40 × magnification, having 4080 pixels × 3072 pixels (1 pixel = 0.0539 μm), and magnified to 160 ×, using Image-Pro Software.

Axon photomicrographs were manually performed with the aid of IS Image-pro version 4.5, consisting of an active area of 220 μm × 165 μm. Experimental and control group slides data, on the same rodent, were analyzed. Each group had 17 animals and 1 slide/animal used for data analysis. Ten 40 × fields from each slide were used for counting. On photomicrographs, outer and inner diameters of each axon were manually traced. The times taken to measure parameters of total axons on one photomicrograph were counted.

Using the manual method, axon calibers and fiber diameters were measured with the aid of Image Pro analyzer software. For each field, analysis was carried out with the following steps: (a) Made a layered image with an appropriate threshold factor (1.00±0.30) depending

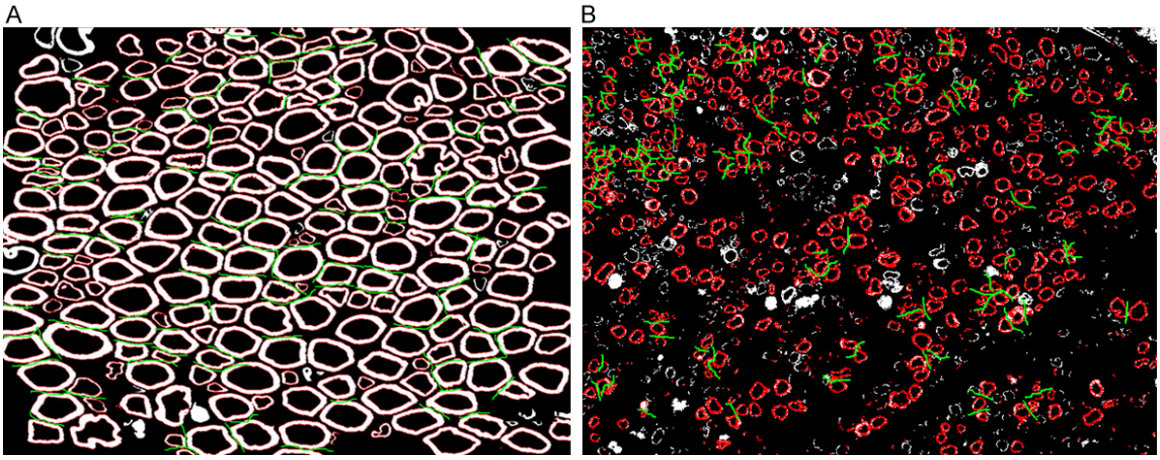

Figure 2. Axon caliber and fibers outer diameter of each axon was semi-automatically traced by using Image Pro analyzer software. Two closely aligned fibers were allowed manually splitting. A: Control Group; B: Experimental Group; 40 ×.

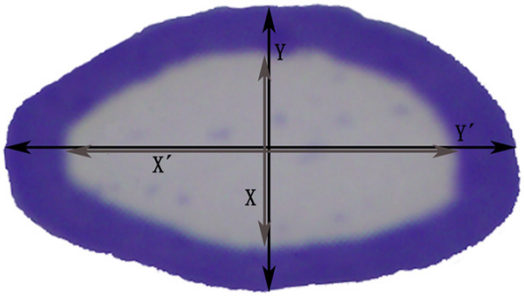

Figure 3. Axon g-ratio analysis model. X: The minimum axon caliber; X': The maximum axon caliber; Y: The minimum fibers outer diameter; Y': The maximum fibers outer diameter.

on the total fibers on the photomicrograph [16]; (b) Made the raw profile and intermediate profile; (c) Kept the original image mask; (d) Split or merged the fibers when two fibers were in close contact with each other or supposed to look like the single axon; (e) Deleted artifactual objects such as blood vessels and perineurium fragments; (f) Selected eligible objects and created a line to mark the lengths of axon caliber and fiber diameter; and (g) Exported data to Excel sheets (**Figures 1** and **2**).

Each axon digitizes 8 arrows. Four light arrows represented the minimum and maximum axon caliber while the other 4 dark arrows indicated outer diameter.

For measurement of g-ratios using manual method (**Figures 3** and **4**), the following formula was utilized [17]:

Axon Caliber: $X_{average} = (X + X')/2$;

Fibers Diameter: $Y_{average} = (Y + Y')/2$;

G-Ratio = $X_{average}/Y_{average}$

Semi-automatic analysis of axon counts, axon calibers, and g-ratios

For semi-automatic analysis of the three parameters, mentioned above, the same procedure was performed to obtain photomicrographs. Axon areas and fiber areas of each axon were semi-automatically traced using Image Pro analyzer software. Software was utilized for the procedures from (a) to (e), mentioned above, in the process of manual measurements (**Figure 2**). Afterward, areas (the myelin sheath area), diameters (mean of fibers outer diameter), and hole areas were automatically measured (**Figures 4** and **5**).

Semi-automatic programs on axon photomicrograph analysis proven with calculus

For measuring axon parameters in the semi-automatic method, the following formula was used:

Axon Caliber = Diameter * G-Ratio

G-Ratio = SQRT (Hole Area/The Area + Hole Area). (SQRT: Square Root.)

To prove that the above formulas were available, methodological explanations are given in the following three sections:

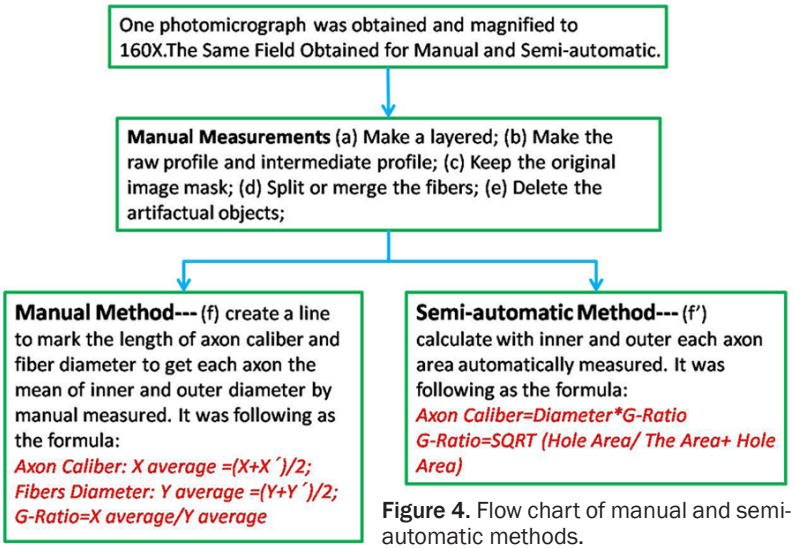

Figure 4. Flow chart of manual and semi-automatic methods.

Homothetic center of two irregular circles figures-based morphometry: One axon photomicrograph was magnified to 640 × under Image Pro software. There were two geometric figures, internal and external, in each axon. The internal or external irregular circle figures respectively digitized 3 points by clockwise with 120°±10° on behalf of the three angles. The internal circle figure randomly digitized 3 points (a', b', c'); the external circle figure respectively digitized the corresponding 3 points (a, b, c), which were homologous points. The lines aa', bb', and cc' drew through two endpoints, which is the homothetic center of those two irregular figures, showing as appoint O (**Figure 6**). Next, to calculate the percentage of these three lines (aa', bb', and cc'), drawing was performed through the same endpoint, the homothetic center of these two irregular circles figures.

Homothetic similarity between internal and external photomicrographs of each axon: In geometry, the center of similarity is a point from which two geometrically similar figures are seen as a dilation or contraction of one another [18, 19]. The two figures are directly similar or scaled mirror images of one another. There was one homothetic center in the control and experimental groups with 92.35% and 82.67%, respectively, in internal and external photomicrographs of each axon. Consequently, more than 80% of axons having internal and external irregular circles photomicrographs with one homothetic center also had homothetic morphometry (**Figure 6**, **Table 1**).

Semi-automatic axon g-ratio analysis based on calculus: Given an irregular circle (IC), tangent lines at A and B were added, respectively. The two lines intersected at the origin in polar coordinate, denoted by O in **Figure 7**. Mean diameter of IC is denoted by 2r. In the polar coordinate, they denoted α and β to be the angle of line OA and line OB, respectively. This study further denoted the curve of the arc AB that was below the line segment AB to be $\varphi_1(\theta)$, and the arc AB that was above the line segment AB to be $\varphi_2(\theta)$, where $\alpha \le \theta \le \beta$. Thus, the area of IC can be computed by double integration in polar coordinate as follows:

$$S(IC) = \int_{\alpha}^{\beta} d\theta \int_{\varphi_1(\theta)}^{\varphi_2(\theta)} r dr = 1/2 \int_{\alpha}^{\beta} (\varphi_2^2(\theta) - \varphi_1^2(\theta)) d\theta \quad (1)$$ [20].

In the previous section, the homothetic similarity between the internal and external photomicrographs of axons was proven, as well as in the case for most axons possessing one homothetic center. This study chose one irregular circle axon, which was a homothetic figure from the control group, to calculate the area including "Hole Area" and "The Area (the myelin sheath area) + Hole Area" by (1). Let us denote S (internal) to be "Hole Area", and denote S (external) to be "The Area + Hole Area". Let 2r' and 2r be "axon caliber" and "fibers outer diameter", respectively (**Figure 8**). As before, the angles of lines OA'A and OB'B were denoted by α and β, respectively. Notations for external IC remained the same, while for internal IC, all notations came with a prime in the subscription.

As these two ICs were similar, for all $\alpha \le \theta \le \beta$, we had $\varphi_1(\theta) = p\,\varphi'_1(\theta)$ and $\varphi_2(\theta) = p\,\varphi'_2(\theta)$ for some constant $p = r/r' \le 1$. Applying (1) we had the followings:

$$S(internal) = \int_{\alpha}^{\beta} d\theta \int_{\varphi'_1(\theta)}^{\varphi'_2(\theta)} r dr = 1/2 \int_{\alpha}^{\beta} (\varphi'^2_2(\theta) - \varphi'^2_1(\theta)) d\theta \quad (2)$$

$$S(external) = \int_{\alpha}^{\beta} d\theta \int_{\varphi_1(\theta)}^{\varphi_2(\theta)} r dr = 1/2 \int_{\alpha}^{\beta} (\varphi_2^2(\theta) - \varphi_1^2(\theta)) d\theta \quad (3)$$

It leads to:

$$\begin{aligned} S(external) &= 1/2 \int_{\alpha}^{\beta} (\varphi_2^2(\theta) - \varphi_1^2(\theta)) d\theta \\ &= p^2/2 \int_{\alpha}^{\beta} (\varphi'^2_2(\theta) - \varphi'^2_1(\theta)) d\theta = p^2\, S(internal) \end{aligned} \quad (4)$$

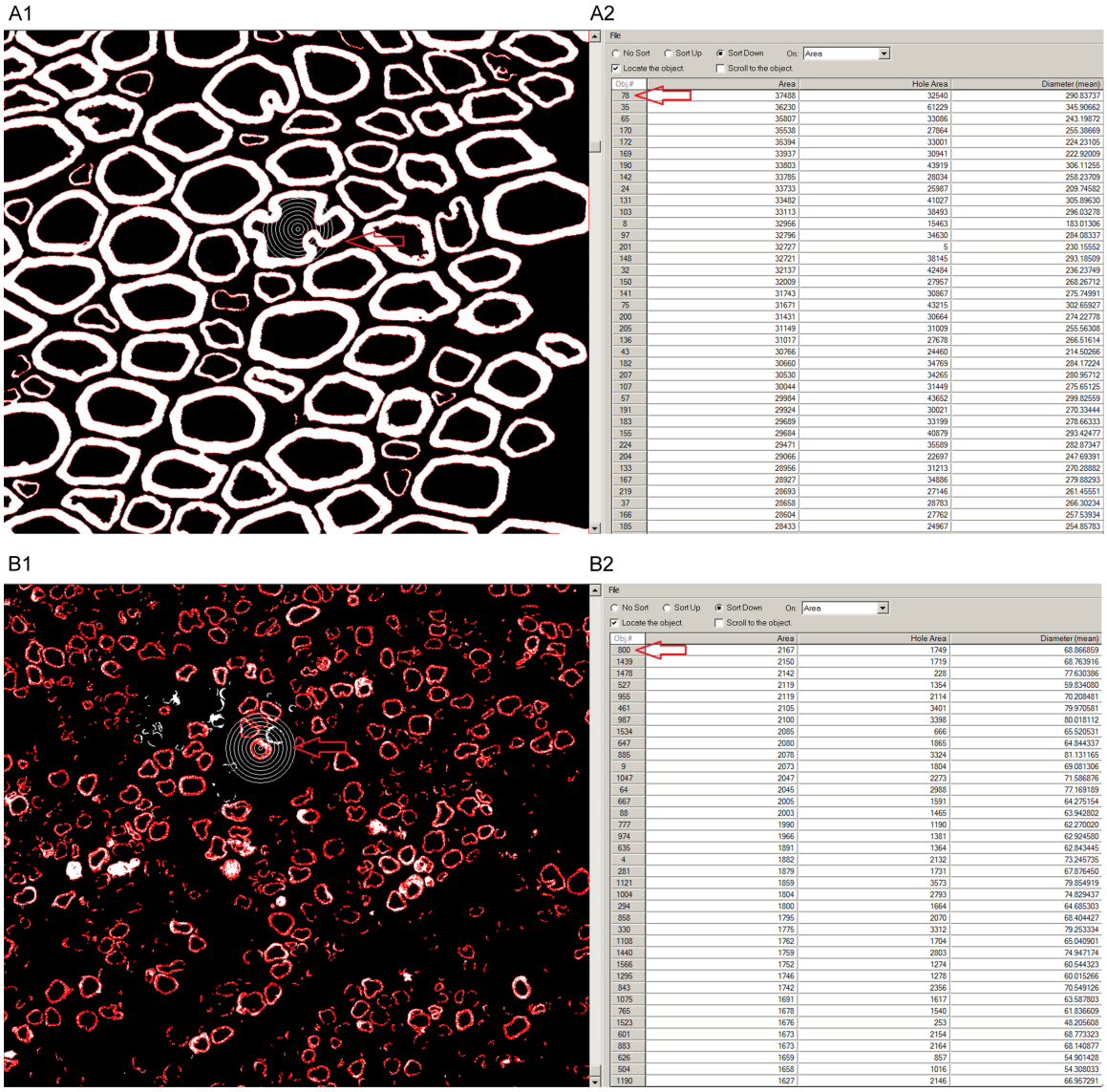

Figure 5. Area (the myelin sheath area), diameter (mean of fibers outer diameter), and hole area on one photomicrograph were automatically measured. A1 and A2: Control Group; B1 and B2: Experimental Group; Arrow: Split of fibers when two fibers were in close contact with each other. 80 ×.

Finally,

$p = \sqrt{S(internal)/S(external)}$ = r/r' = Axon caliber/Fibers outer diameter = $X_{average}/Y_{average}$

This has proven the measurement of g-ratios using the formula as SQRT (Hole area/The Area + Hole area).

The same field obtained for manual measurement and semi-automatic analysis

All measurements were made by a single skilled observer blinded to photomicrographing. Parameters from the photomicrographs were taken and analyzed by the same observer for both methods (**Figure 9**). Procedures of the manual method and semi-automatic analysis were respectively followed, as mentioned previously. Values on the same field, obtained from two methods, were compared and analyzed.

Statistical analyses

Paired t-tests with a significance level of $P<0.05$ were used for statistical analysis of differences between the following groups: 1) Mean duration for performing both methods (manual and semi-automatic methods) and 2) Axon caliber and g-ratio values on the same photomicrograph obtained using both methods. Axon count values on the same photomicrographs

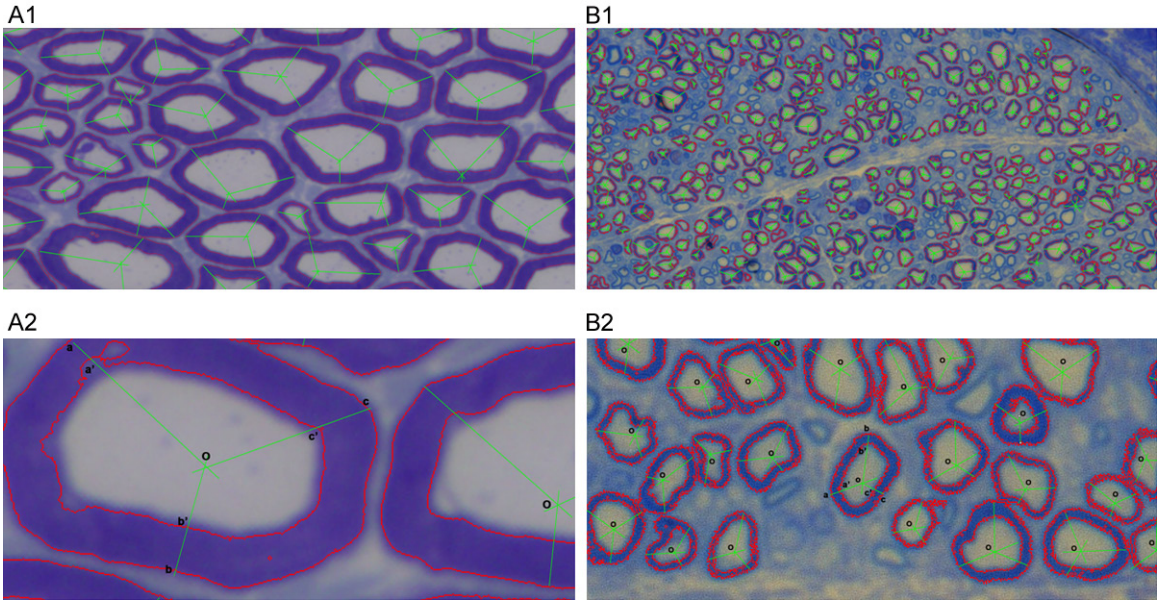

Figure 6. Homothetic similarity between internal and external photomicrographs of each axon The internal circle figure random digitizes 3 points (a', b', c') with 120°±10°; the external circle figure respectively digitizes corresponding 3 points (a, b, c). The line aa', bb' and cc' draw through an endpoint which is homothetic center of those two irregular figures and showed as a point O. A1 and A2: Control Group; B1 and B2: Experimental Group; A1 and B1: 160 ×; A2 and B2: 640 ×.

Table 1. Two geometric figures possess a homothetic center (%)

Group (n = 170 fields)	One homothetic center/field	More than one homothetic center/field
Control group	92.35%	7.65%
Experimental group	82.67%	17.33%

were obtained using both methods. Data was compared by unpaired t-test. Statistical analysis of differences between the two methods was done with the Bland-Altman method and Pearson's correlation was used to assess the relationship between the two methods [21-23]. Bland has suggested that a sample of 100 measurements was adequate, in most cases. Sample size for this present study exceeded this number [24]. Continuous data are presented as mean ± SD. All calculations were done using Prism software (Graph Pad Inc., La Jolla, CA).

Results

Comparison of axon count, axon caliber, and g-ratio analysis in the same field between manual and semi-automatic methods

A total of 17 rats from 170 fields were included in the analysis. **Table 2** and **Figure 10** show the

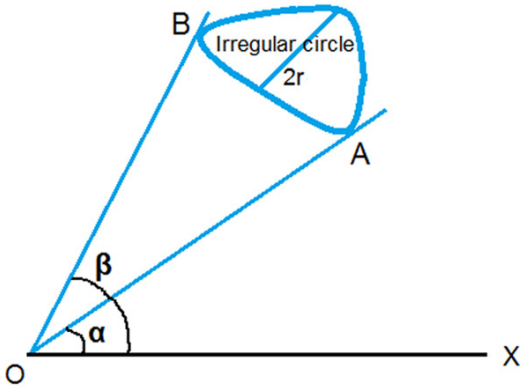

Figure 7. Irregular circle in polar coordinate. The point O, the origin of coordinates, is an intersection for the two tangents OA and OB. The angles of lines OA and OB are denoted by α and β. Denoting the mean of diameter irregular circle by 2r.

results of three parameter values obtained from manual and semi-automatic methods. The assumption for comparison was fulfilled: differences (semi-automatic-manual counting) against the averages (semi-automatic + manual)/2 (**Figure 10A1-C2**). Bland-Altman image analysis showed that axon counts obtained using the semi-automatic method were quite similar to that obtained using manual counting. Variances of axon caliber and g-ratio values calculated with both methods were statistically equal.

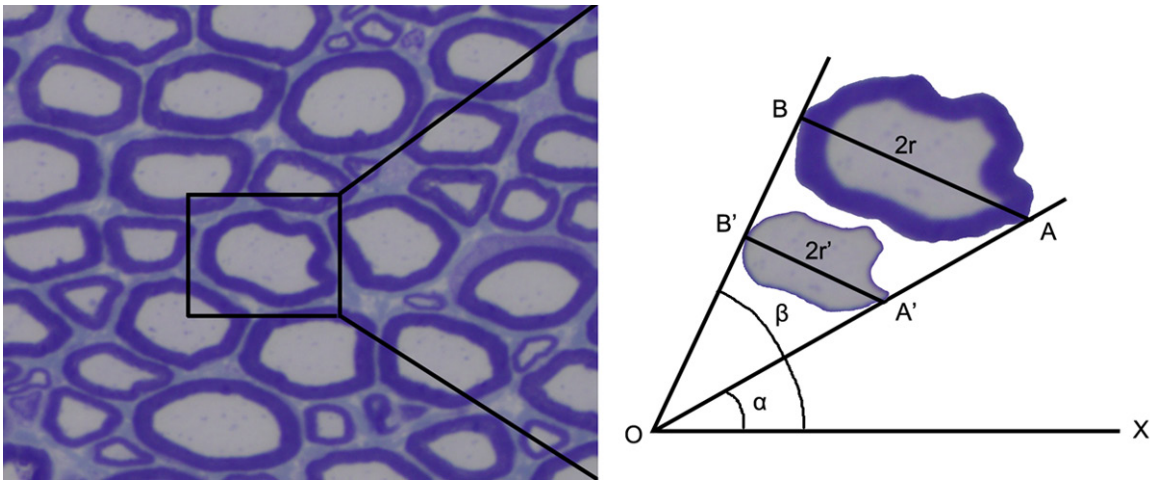

Figure 8. Internal and external photomicrographs in polar coordinate. The internal and external photomicrographs of one axon were separated to two irregular circles which has a homothetic center O. The points A and A' are homologous, as are the point band B'. The mean diameter of the circles was showed as 2r and 2r' respectively. The area of internal figure (Hole Area) and external figure (The Area + Hole Area) were represented as S(internal) and S(external) respectively.

Pearson's correlation coefficient for axon calibers in the control and experimental groups was 0.8934 (P<0.001) and 0.6971 (P<0.001), separately for manual and semi-automatic methods. For axon g-ratio, it was 0.8765 (P<0.001) and 0.9824 (P<0.001) between the two methods (**Table 3**). These results suggest that the semi-automatic method is just as accurate as the manual method.

Time taken to perform on the same field for manual analysis and semi-automatic analysis

Average time spent on calculating fiber outer diameters and axon calibers are shown in **Table 4** and **Figure 11**. Manual axon measurements took more than 2 hours to harvest the values. In the same field, with semi-automatic measurements, values were acquired and their analysis required about 1 hour. There was a significance difference (P<0.001) between mean time of durations between manual and semi-automatic measurements.

Discussion

This present study aimed to demonstrate that the semi-automatic method of axon measurement is more effective, efficient, accurate, and easier to perform than the manual approach. This study deducted and presented the formula implemented into the semi-automatic method. To reliably compare results of axon measurements, including their accuracy and time needed to get and to analyze them, this study conducted axon measurements both semi-automatically and manually, using the same sample slides, with a statistically representative number of 50. Manual in-depth analysis of such a large number of slides is extremely time consuming and exhausting, with vulnerability to human mistakes (e.g. right sequence of measurement, correct match between the inner and outer diameter). Mistakes during the process might lead to time-consuming corrections or a need to redo the entire process.

Other reports of semi-automatic analysis systems have shown that focusing on only one shape and size in the analysis of myelin during nerve regeneration can be time-saving [11]. This method was applicable to morphologically normal and apparently axonal shape and size homogeneity nerves. Some judgments and differentiation can't be done by a completely automated system, such as evaluating the parameters of nerves with irregular shapes or more complex patterns of regeneration on current sources. It should be realized that fully automated tools would be almost impossible with our existing technology. This present semi-automatic method is more resistant to these types of errors, as it is based not only on manually assisted precise recognition of target objects, but also on automatic measurements of the corresponding area. Therefore, the semi-automatic method compensates for shortcom-

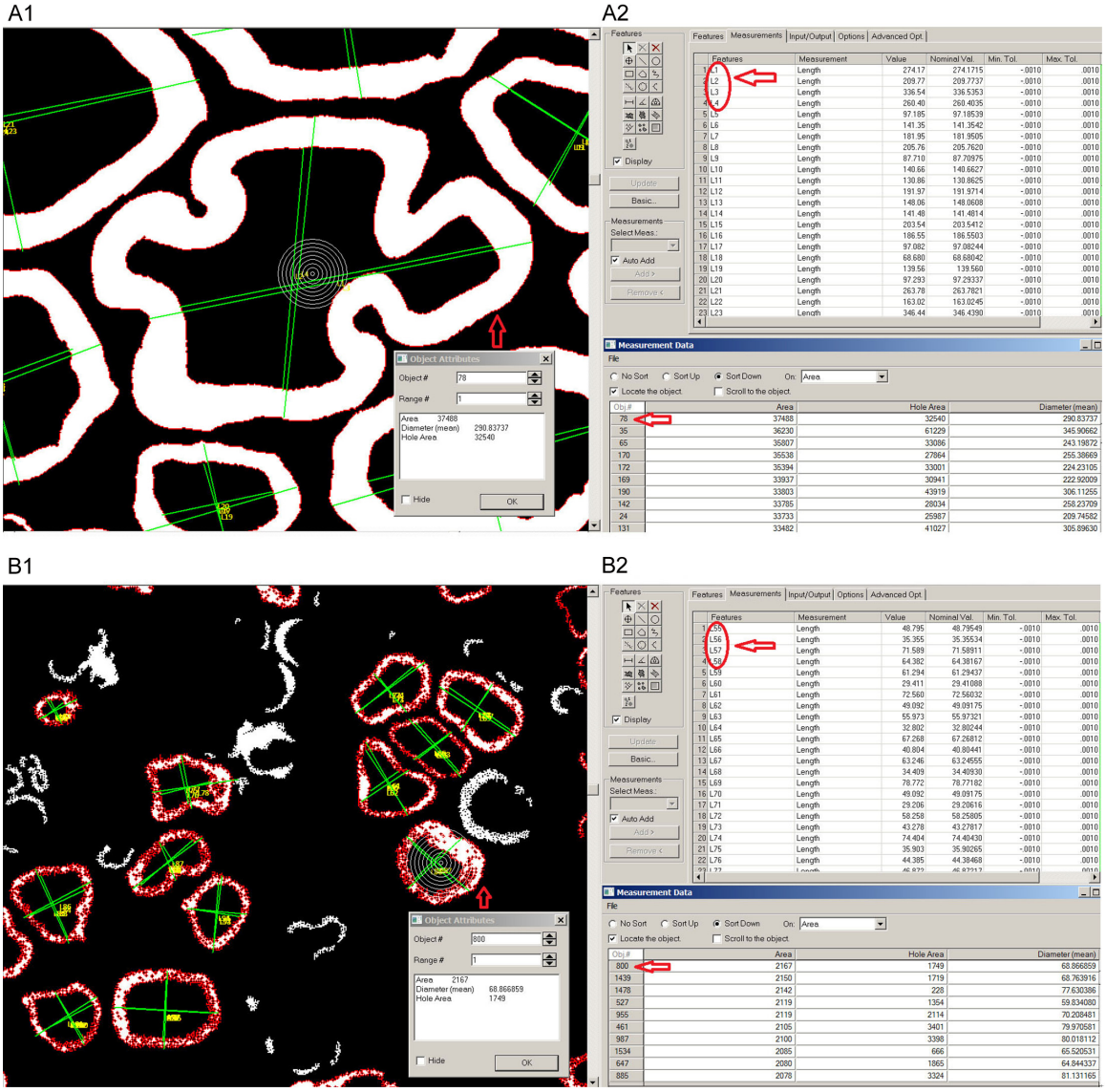

Figure 9. Using manual and semi-automatic methods to calculate g-ratios on the same Photomicrograph. A1 and A2: Control groups; B1 and B2: Experimental groups. A1 and B1: red arrow shows N0.78 axon and N0.800 axon, respectively; Upper of A2 and B2: Axon inner caliber and outer diameter from manual method. The length of L1-L4 is attributed to N0.78 axon and L55-L58 belongs to N0.95 axon, respectively. Below of A2 and B2: The Area, diameter and Hole Area on one photomicrograph were automatically measured from semi-automatic methods. 320 ×.

Table 2. Axon count, axon caliber, and g-ratio values obtained with manual and semi-automatic methods (mean ± SD)

Groups	Axon counts		Axon caliber (μm) (170 fields)		Axon g-ratio (170 fields)	
	Semi-automatic	Manual	Semi-automatic	Manual	Semi-automatic	Manual
Control group	368.6±106.4 (n = 17)	399.2±77.18 (n = 17)	5.504±1.745	5.634±2.148	0.5695±0.066	0.5685±0.054
Experimental group	287.1±7 8.32 (n = 34)	314.3±49.92 (n = 34)	3.448±1.379	3.319±1.356	0.6672±0.076	0.6659±0.079

Note: There were no significant differences between results of axon counts, axon caliber, and axon g-ratio obtained using manual and semi-automatic methods by the unpaired t-test (for axon counts) or paired t-test (for axon caliber and axon g-ratio).

ings in software analysis and improves the efficiency and accuracy of analyzing sections with damaged and more complex patterns of regenerative nerves.

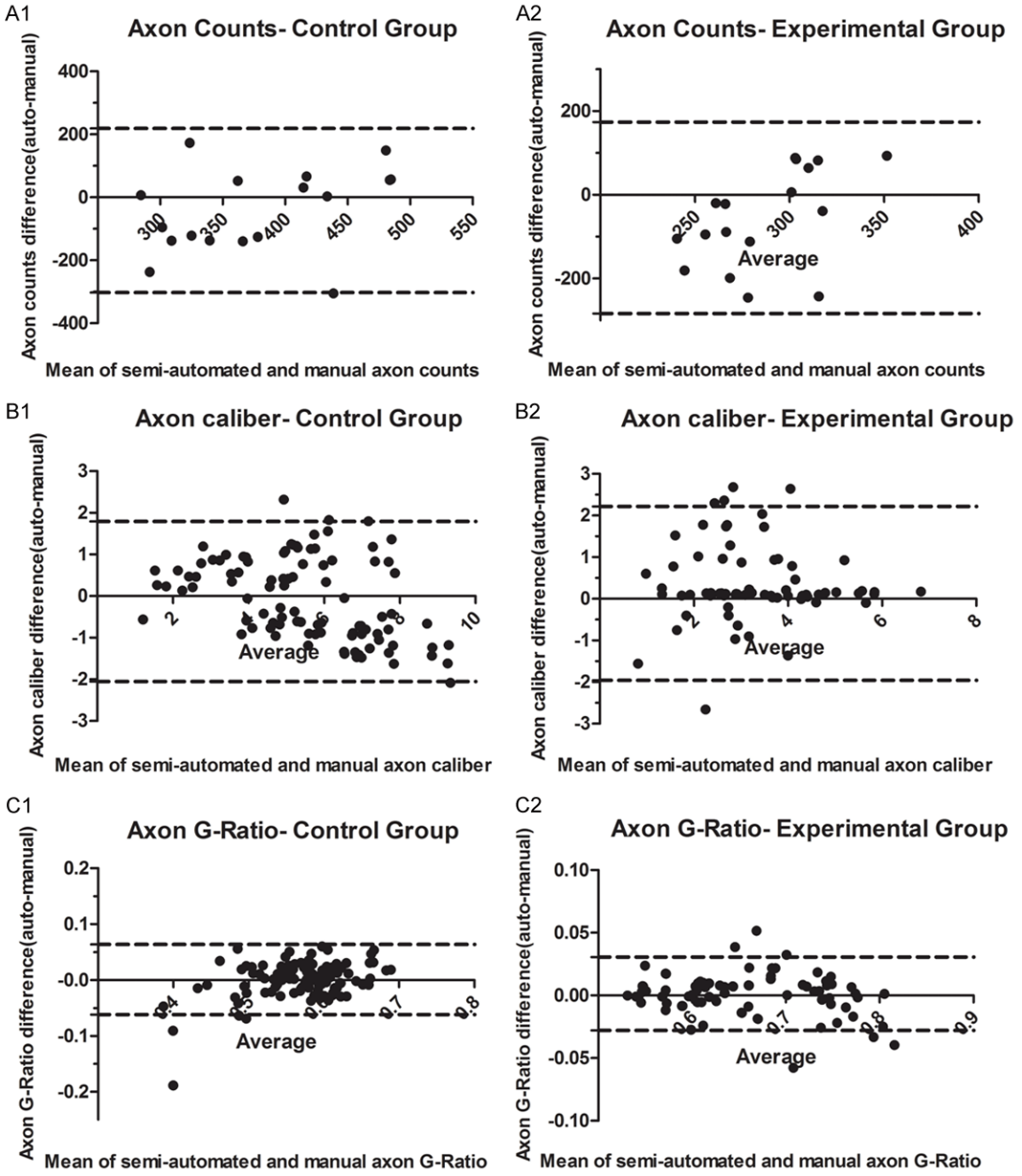

Figure 10. Bland-Altman plots of axon parameters between manual and semi-automatic methods. Bland-Altman plots of Axon Counts between the manual and semi-automatic methods (A1, A2); Bland-Altman plots of Axon Caliber between the manual and semi-automatic methods (B1, B2); Bland-Altman plots of G-Ratio value between the manual and semi-automatic methods (C1, C2); The difference (e.g., Axon Counts by semi-automatic Method-Axon Counts by manual method) was plotted against the average of both assessments (e.g. (Axon Counts by semi-automatic method + Axon Counts by manual method)/2). Solid reference lines represent the mean difference; the dotted lines indicate ±2 SD about the mean.

Importantly, the results of axon counts, variance of axon calibers, and g-ratio values were statistically equal using semi-automatic and manual method (Bland-Altman method and the Pearson's correlation analysis). Time needed to obtain results with the semi-automatic method was less than half that of the manual method. Thus, this study proposed the semi-automatic

Table 3. Pearson's correlation coefficient (r)

	Axon caliber (μm) (170 fields)		Axon g-ratio (170 fields)	
	Control group	Experiment group	Control group	Experiment group
Semi-automatic vs. manual	0.8934 (P<0.001)	0.6971 (P<0.001)	0.8765 (P<0.001)	0.9824 (P<0.001)

Table 4. Mean time durations obtained with manual and semi-automatic methods for calculating fibers outer diameter and axon caliber

Group (n = 170 fields)	Semi-automatic analysis (min/field)	Manual analysis (min/field)	Time saving (%)
Control group	62.63±8.665*	138.8±12.48	54.89
Experimental group	71.22±10.19*	158.1±15.54	54.95

Note: There was a significance difference between results obtained using the manual and semi-automatic methods by paired *t-test*. *Compared to manual method P<0.001.

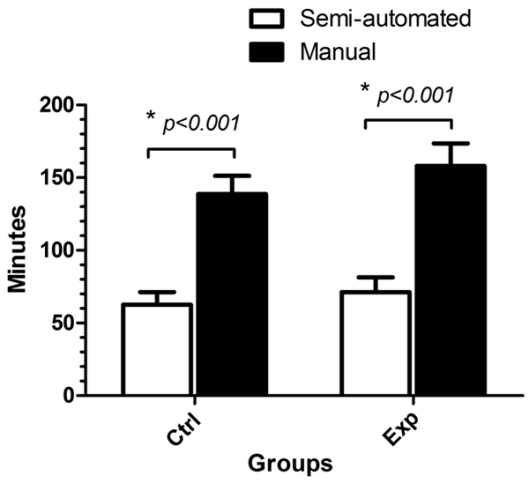

Figure 11. Time durations performed in the same field using manual and semi-automatic methods. There was a significance difference between time durations obtained using the manual and semi-automatic methods by paired t-test. (*Compared to manual method P<0.001). Ctrl, control group; Exp, experimental group.

method which allows obtaining measurements in 50% of the time needed for manual measuring.

One limitation of this study was the fact that there was more than one homothetic center in control and experimental groups, with 7.65% and 17.33%, respectively. The myelinated fiber profile was not always represented as homogeneous. The reason might be that the smaller axonal fibers, hard to stain or strongly heterogeneous, were considered difficult to mark by 3 points. In the experimental group, regenerated axons might be of a grotesque shape rather than of a regular circle. Thus, some axons are expected to have more than one homothetic center in the same fiber.

Area of axon and fibers obtained from the semi-automatic method was used to calculate the axon g-ratio. By "SQRT (Hole Area/The Area + Hole Area)" formula, average value for g-ratios in the same field was not showing any statistically significant difference, compared to that obtained from manual methods. Since it has also been proven that in homothetic irregular circles SQRT (S(internal)/S(external)) is equal to axon caliber/fibers outer diameter, which is the g-ratio of an axon (2)-(4), the formula "SQRT (Hole Area/The Area + Hole Area)" can yet be regarded as another way to figure out axon g-ratio in peripheral nerves.

Average analysis g-ratio time using the semi-automatic method for sciatic nerve transections, containing about 400-700 fibers in one field (40X), was comparable to that of another semi-automatic technique [9]. Moreover, it was found that with the semi-automatic method, many fibers can be rapidly counted after automatic segmentation. Adjustment of threshold is rarely necessary if nerve sections are of good quality. Hence, the semi-automatic method demonstrated improved efficiency, as much as possible, while maintaining a similar level of accuracy, providing extremely productive results.

In conclusion, this study introduced a highly efficient semi-automatic method for measuring axon counts, axon calibers, and g-ratios.

Acknowledgements

This study was supported by the National Natural Science Foundation of China (NSFC) (No.81672247 to Yan Wo), NSFC (No.81402618 to Zhen Zhang), NSFC (No.81571835 to Kan Wang), Natural Science Foundation of Shanghai Project (No.15ZR1405000), Innovation Program of the Shanghai Municipal Education Commission (No.15ZZ006), and CAS Key La-

boratory of Nano-Bio Interface (No.17NBI01 to Jun Chen).

Disclosure of conflict of interest

None.

Address correspondence to: Yan Wo, Department of Anatomy and Physiology, School of Medicine, Shanghai Jiao Tong University, No.227 South Chongqing Road, Shanghai City 200025, China. Tel: +86-021-63846590; E-mail: woyan6539@163.com; Jun Chen, Department of Orthopaedic Sports Medicine, Huashan Hospital, Fudan University, No. 12 Urumqi Middle Road, Shanghai City 200040, China; CAS Key Laboratory of Nano-Bio Interface, Suzhou Institute of Nano-Tech and Nano-Bionics, Chinese Academy of Sciences, No.398 Ruoshui Road, Suzhou 215028, Jiangsu Province, China. Tel: +86-021-52889999; E-mail: chenjunv5d@163.com

References

[1] Schmalbruch H. Fiber composition of the rat sciatic nerve. Anat Rec 1986; 215: 71-81.
[2] Rushton WA. A theory of the effects of fibre size in medullated nerve. J Physiol 1951; 115: 101-22.
[3] de Campos D, Xavier LL, Goulart GR, Thomaz LD, Malysz T, Jotz GP. Similarities in the surface area/volume ratio in the fibers of the recurrent laryngeal nerve can explain the symmetry in the vocal fold mobility? Med Hypotheses 2015; 85: 989-91.
[4] de Campos D, Heck L, Jotz GP, Xavier LL. Degree of myelination (g-ratio) of the human recurrent laryngeal nerve. Eur Arch Otorhinolaryngol 2014; 271: 1277-81.
[5] Carriel V, Garzón I, Alaminos M, Cornelissen M. Histological assessment in peripheral nerve tissue engineering. Neural Regen Res 2014; 9: 1657-60.
[6] Romero E, Cuisenaire O, Denef JF, Delbeke J, Macq B, Veraart C. Automatic morphometry of nerve histological sections. J Neurosci Methods 2000; 97: 111-22.
[7] Ewart DP, Kuzon WM, FiSh JS, McKee NH. Nerve fibremorphometry: a comparison of techniques. J Neurosci Methods 1989; 29: 143-50.
[8] Friede RL, Beuche W. Combined scatter diagrams of sheath thickness and fibrecalibre in human sural nerves: changes with age and neuropathy. J Neurol Neurosurg Psychiatry 1985; 48: 749-56.
[9] Mezin P, Tenaud C, Bosson JL, Stoebner P. Morphometric analysis of the peripheral nerve: advantages of the semi-automated interactive method. J Neurosci Methods 1994; 51: 163-9.
[10] McCreedy DA, Margul DJ, Seidlits SK, Antane JT, Thomas RJ, Sissman GM, Boehler RM, Smith DR, Goldsmith SW, Kukushliev TV, Lamano JB, Vedia BH, He T, Shea LD. Semi-automated counting of axon regeneration in poly (lactide co-glycolide) spinal cord bridges. J Neurosci Methods 2016; 263: 15-22.
[11] da Silva AP, Jordão CE, Fazan VP. Peripheral nerve morphometry: comparison between manual and semi-automated methods in the analysis of a small nerve. J Neurosci Methods 2007; 159: 153-7.
[12] Auer RN. Automated nerve fibre size and myelin sheath measurement usingmicrocomputer-based digital image analysis: theory, method and results. J Neu-rosci Methods 1994; 51: 229-38.
[13] Romero E, Cuisenaire O, Denef JF, Delbeke J, Macq B, Veraart C. Automaticmorphometry of nerve histological sections. J Neurosci Methods 2000; 97: 111-22.
[14] Vita G, Santoro M, Trombetta G, Leonardi L, Messina CA. Computer-assisted auto-matic method for myelinated nerve fiber morphometry. Acta Neurol Scand 1992; 85: 18-22.
[15] Savy C, Margules S, Solari A, Saint-Jean P, Farkas-Bargeton E. An image analysismorphometric method for the study of myelinated nerve fibers from mousetrigeminal root. Anal Quant Cytol Histol 1988; 10: 307-16.
[16] More HL, Chen J, Gibson E, Donelan JM, Beg MF. A semi-automated method for identifying and measuring myelinated nerve fibers in scanning electron microscope images. J Neurosci Methods 2011; 201: 149-58.
[17] Rushton WA. A theory of the effects of fibre size in medullatednerve. J Physiol 1951; 115: 101-22.
[18] Johnson RA. Modern geometry: an elementary treatise on the geometry of the triangle and the circle. Boston, MA: Houghton Mifflin 1929.
[19] Bruce EM. Fundamental concepts of geometry, chapter 5-6 homothetic transformations. Addison-Wesley Publishing Company 1955; 166-169.
[20] Thomas GB Jr, Weir MD, Hass JR. Thomas's Calculus, Multivariable (12th edition). Pearson 2009.
[21] Bland JM, Altman DG. Comparing methods of measurement: why plotting difference against standard method is misleading. Lancet 1995; 346: 1085-7.
[22] Bland JM, Altman DG. Measuring agreement in method comparison studies. Stat Methods Med Res 1999; 8: 135-60.
[23] Lu MJ, Zhong WH, Liu YX, Miao HZ, Li YC, Ji MH. Sample size for assessing agreement between two methods of measurement by bland-altman method. Int J Biostat 2016; 12.
[24] Bland JM, Altman DG. The logranktest. BMJ 2004; 328: 1073.